JOURNAL OF MATERIALS SCIENCE 21 (1986) 2781–2786

Some observations on dendritic arm spacing in Al–Si–Mg and Al–Cu alloy chill castings

M. BAMBERGER, I. MINKOFF, M. M. STUPEL
Department of Materials Engineering Technion, Israel Institute of Technology, Haifa 32000, Israel

The heat flux from a cast cylinder to a steel chill was experimentally determined for a commercial Al–Si–Mg alloy (A356) and for Al–Cu alloys having different copper contents. The relationship between variation of the heat flux with time, initial temperature of the chill, and solute concentration was determined. The heat flux from the casting to the chill in the A356 alloy is higher than in an Al–7.5% Si alloy, but the microstructure of the former is coarser. The time dependence of the heat flux in an Al–Cu alloy is similar to that in A356 and in Al–7.5% Si. Calculated values for the temperature of the casting and the local solidification time as functions of the distance from the chill were obtained with the aid of the heat flux data and a program for calculating the temperature field during solidification. A good fit with experimental measurements was achieved. Measurements of the mean secondary dendritic arm spacing at different distances from the chill resulted in the relationship $\lambda = at_f^{0.43}$ between the local solidification time (t_f) and the dendtitic arm spacing (λ), where a is a characteristic of the alloy and of the solute concentration. It is noted from the results that the λ value depends not only on the solidification time but also on the concentration of solute element. Different aspects of the evolution of structure, and some attention to growth with high temperature gradients in the presence of chill is discussed.

1. Introduction

When casting aluminium alloys for high strength purposes it is customary to prevent the formation of shrinkage cavitites by local chilling. The rates of chilling and of solidification are characteristic of the local solidification conditions, and these in their turn have an important effect on the local microstructure. The higher the rate of solidification, the finer the resulting microstructure. The relationship between the local solidification time, t_f, and the dendritic arm spacing, λ, is represented by [1]

$$\lambda = at_f^n \qquad (1)$$

where a and n are constants. For secondary arm spacing $0.3 < n < 0.5$ with most values close to 0.3. In a previous study [2] the heat flux from an Al–Si alloy to a steel chill (without ceramic coating) was determined for different silicon contents and different initial temperatures using a numerical solution, with the aid of a computer program, of the time-dependent heat conduction equation. The solution is based on measuring the temperature at a point in the chill close to the casting-chill interface. Fig. 1 shows, as an example, the heat flux from the casting to the chill in an Al–7.5 wt % Si alloy, for two initial chill temperatures.

A further computer program, based on the heat flux (as shown in Fig. 1), was utilized for calculating the temperature field in the course of solidification. In some cases a comparison was made between the temperature field measured in the casting and that calculated; a good fit was obtained, confirming the reliability of the method. These calculations yielded the time lapse between the liquidus and solidus temperatures, i.e. the local solidification time, as a function of the distance from the chill. Simultaneously the mean dendrite arm spacing was measured, also as a function of the distance from the chill. In this manner the relationship between the dendrite arm spacing and the local solidification time could be determined for different silicon contents (Fig. 2). The result is a dependence similar to that given in Equation 1, but the value of the exponent is higher than is normally determined, and in the experiments described here $n = 0.43$. It was also observed that in the case of aluminium alloys of both silicon and copper, the higher the solute content the finer was the observed microstructure at a constant local solidification time.

2. Experimental procedures

The A356 alloy used in this reasearch is marketed by Alcan Lynemouth Ltd (Ashington, UK). Its composition, determined by spectroscopy is shown in Table I. The Al–Cu alloy was based on the commercial 2024 alloy, to which pure aluminium and pure copper were added in order to obtain the compositions shown in Table I. The metal was cast into a sand mould containing a steel chill of 100 mm diameter and 40 mm thickness. A cylinder-shaped casting was obtained, having a diameter of 80 mm and a height of 60 mm. The entire cast cyclinder was located over the steel chill, so that the cooling and solidification

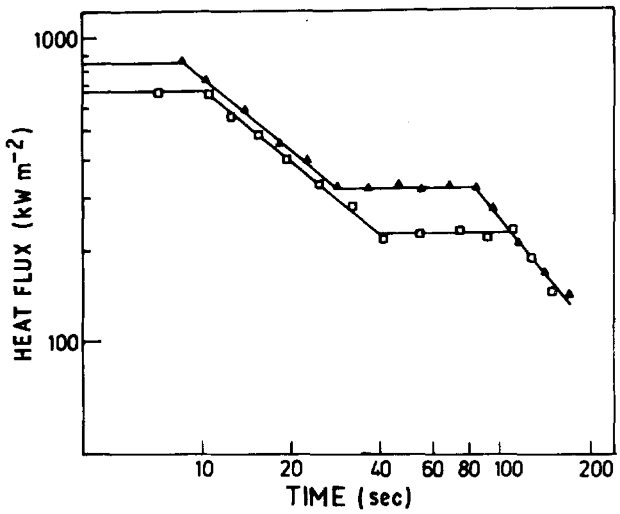

Figure 1 Heat flux as a function of time for Al–7.5% Si. The results for two chill temperatures are shown: (△) 20° C, (□) 250° C.

rates depended for the most part on the distance between location in the casting and the chill. The temperature in the course of solidification was measured at ten points in the chill, all at a distance of 4 mm from the interface with the casting and a schematic representation of the casting system is shown in Fig. 3.

The measurements were fed into the computer, to obtain the heat flux from the casting to the chill [2]. The simultaneous measurement of the temperature at ten different points during every experiment generates a large number of parallel results, all independent of each other, and ensures a good accuracy of the calculated heat flux. The latter, as a function of the time that has elapsed since the mould was filled, was fed into another computer program, designed to solve the problem of the solidification of a symmetrical cylindrical body. The program in question takes account of the heat flux from the casting to the chill and to the sand surrounding the casting, the latent heat of solidification, and various thermophysical properties of the casting in both the solid and the molten state [2].

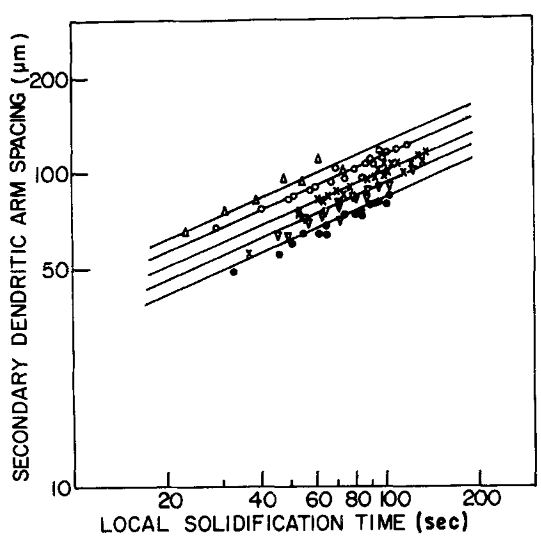

Figure 2 The dendritic arm spacing as a function of the local solidification time in Al–Si alloys, for different silicon contents. (△) 1.0 wt %, (○) 3.8 wt %, (×) 5.7 wt %, (▽) 7.5 wt %, (●) 9.7 wt %.

TABLE I Composition of the alloys examined (in wt %)

	Si	Cu	Fe	Mn	Mg	Ti
Al–7.5% Si	7.5	–	0.51	–	0.06	0.05
A356	6.8	–	0.25	–	0.31	0.14
	0.13	3.5	0.26	0.49	1.11	–
Al–Cu	0.26	4.6	0.22	0.66	1.32	–
	0.1	9.0	0.2	0.61	1.44	–

Comparison was made between the calculated and measured temperatures in the casting using Chromel–Alumel thermocouples of 0.3 mm diameter. These were glass coated, with unprotected hot junctions, and located as in Fig. 3. The temperatures were recorded using Data Logger 10 instrument (Accurex, Mountain View, California), taking readings every 2 sec. The temperature field at different points in time yields the local solidification time as a function of the distance from the chill. On metallographic specimens taken along the cylinder axis at different distances from the chill, the mean dendritic arm spacing was determined. From these values the interdependence of the local solidification time and the dendritic arm spacing can be established, the chemical composition serving as parameter.

3. Results

3.1. Al–Si–Mg (A356)

The A356 alloy was cast over a steel chill (without ceramic coating) having initial temperatures of 20, 110 and 225° C, respectively. The heat flux as a function of time and with the chill temperature is shown in Fig. 4. At the start of solidification there is some delay in the response of the measurement system due to the distance of the point of measurement from the casting–chill interface and because of the response times of the sensors and the recorders. The heat flux in the first part of the measured regime was estimated up to a time interval of 10 sec. After about 12 sec a drop in the

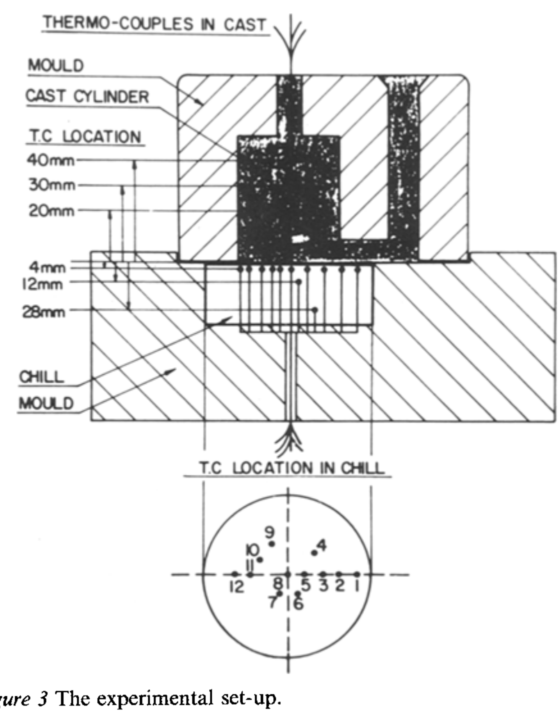

Figure 3 The experimental set-up.

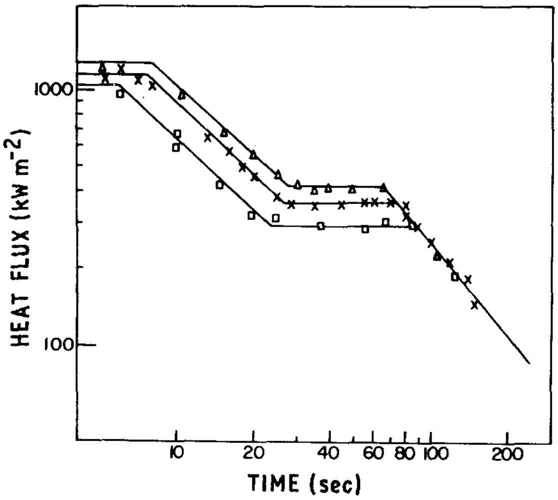

Figure 4 Heat flux as a function of time for a commercial A356 alloy, for three initial chill temperaturs. (△) 20° C, (×) 110° C, (□) 225° C.

heat flux with time becomes apparent as a result of the rise in the temperature of the chill. The character of the curve is similar for all three initial chill temperatures. A comparison between Figs 1 and 4 points to a similar dependence of the heat flux on time, although it is somewhat greater in the A356 alloy. On the basis of these results the temperatures in the casting

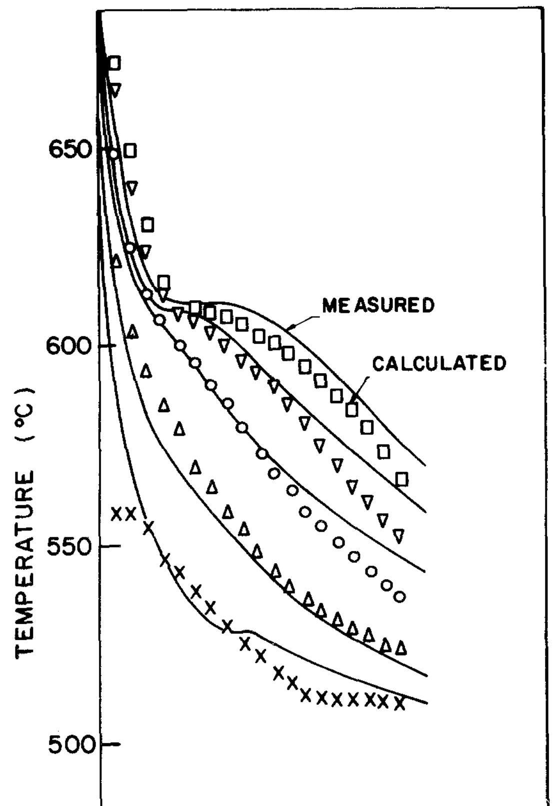

Figure 5 Comparison between the measured and the calculated temperature at various distances from the cast–chill interface as a function of time for A356, initial chill temperature 20° C. (×) surface, (△) 10 mm, (O) 20 mm, (▽) 30 mm, (□) 40 mm.

at various distances from the chill were calculated, and a good fit was found between the calculated and the measured data (Fig. 5). The temperature field allows the calculation of the local solidification time as a function of distance from the chill. Fig. 6 shows the characteristic structure obtained in casting A356 and Al–7.5% Si alloys having equal local solidification times. Differences in the fineness of the primary phase and of the eutectic are clearly discernable. The dendrite arm spacings are shown in Fig. 7, which demonstrates the difference in the fineness of the structures of A356 and Al–7.5 wt % Si with local solidification times in the range of 20 to 80 sec.

3.2. Al–Cu

Al–Cu alloys having copper contents of 3.5, 4.6 and 9.0 wt %, respectively, were cast against a steel chill (without ceramic coating) having initial temperatures of 20 and 250° C, respectively. The heat flux to the chill as a function of time, with the initial temperature of the chill as parameter, is seen in Fig. 8. In these cases the heat flux in very short cooling times had to be estimated. It is clearly seen that the heat flux in this type of alloy is higher than in Al–7.5 wt % Si, but the time dependence is similar. Here, too, deviations of temperature calculated from those measured (in control tests) did not exceed 2 to 3%. By a procedure substantially similar to that previously described the dependence of the dendritic arm spacing on the local solidification time was obtained (Fig. 9). This figure also shows that the higher the solute content, the finer the microstructure, at a constant solidification time.

4. Analysis of results

Accelerated cooling of Al–Si and Al–Cu alloys by means of a metal chill is characterized by a high heat flux at the start of cooling. The pertinent quantity of heat is absorbed in a region close to the interface between the casting and the chill. During this stage, when good contact exists between casting and chill, the heat flux depends on the thermal diffusivity of the casting and its temperature. The thermal diffusivity and the liquidus temperature of Al–Cu are higher than those of Al–Si at equivalent compositions, so that the heat flux at the start of solidification is higher for Al–Cu. This results in a higher interface temperature between casting and chill for Al–Cu, and the temperature gradient in the chill is consequently steeper.

This mechanism is operative as long as heat is absorbed at the top of the chill and close contact exists between the bottom of the casting and the top of the chill. It therefore suffices for determining the heat flux after a relatively short time (12 sec), when the temperature of the top of the chill stabilizes [2]. At this stage the heat flux is determined by the temperature gradient between the casting–chill interface and the centre of the chill. The greater the difference in temperature, the higher the heat flux. The heat flux decreases with time consequent upon the temperature rise in the centre of the chill, while the casting–chill interface temperature remains constant. Since the change in the liquidus temperature of an Al–Cu alloy

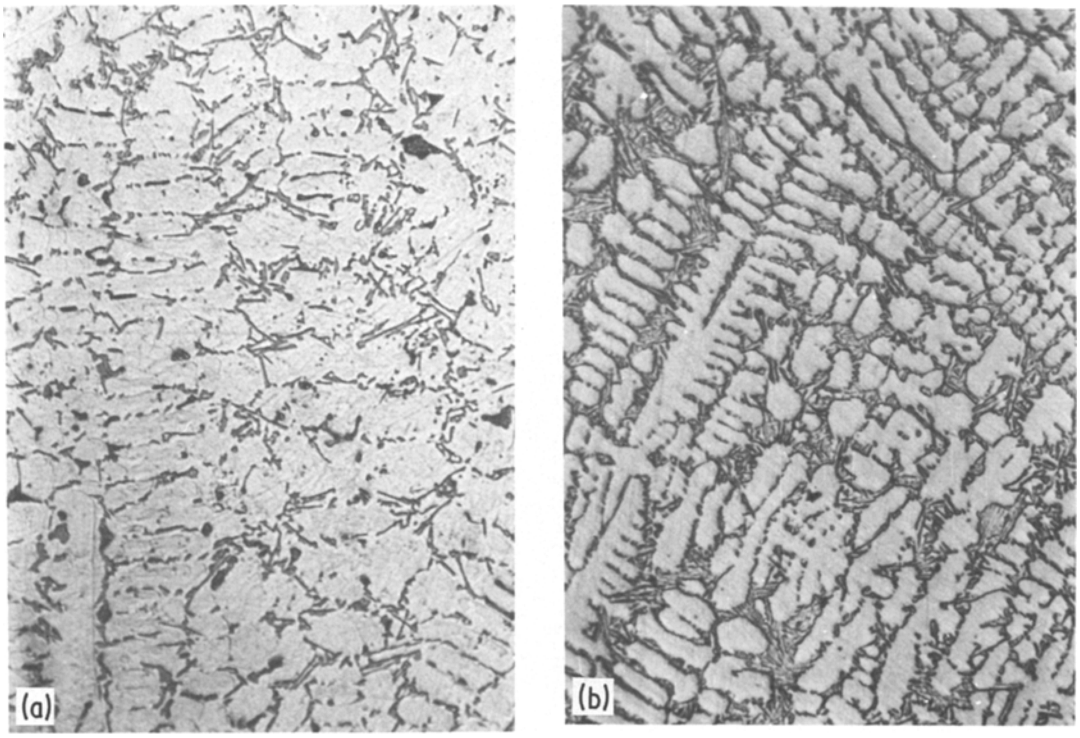

Figure 6 Characteristic structures of (a) A356 and (b) Al–7.5% Si with equal local solidification times (× 60).

as a result of a change in the copper content is small [3] no difference was noted in the heat flux when the copper content was altered in the range of alloys examined here. On the other hand, it was found [2] that an increase in the silicon content in an Al–Si alloys reduced the heat flux to the chill, because the liquidus line in Al–Si is relatively steep, indicating a sharp drop in liquidus temperature as the solute concentration rises. The heat flux curves for Al–Si and Al–Cu alloys therefore show two different types of behaviour. In the former a horizontal portion of constant heat flux is noted. In the latter the heat flux varies continuously with time, being smaller with increasing time intervals. We suggest that this could be due to the eutectic solidification at the lower part of the ingot. By comparison with the time at which the horizontal portion of the heat flux curve occurs, and the temperature as recorded (Fig. 5), it appears that the temperature of the metal near the mould (distance up to 30 mm) is close to the eutectic. From Fig. 5 it can be seen that after 50 sec the solidification front is 30 mm above the chill–casting interface, and at the same time the heat flux decreases (Fig. 4). With the completion of solidification of the lower half of the cylinder, casting and chill become disconnected and cooling takes place by radiation and convection through the air gap between them.

Furthermore, it was found that an increase in the concentration of an alloying element leads to a finer structure. This was also observed in other studies [2, 4]. The dendrite arm spacing in an Al–Si alloy changes from 101 μm with a local solidification time of 80 sec when the silicon content is 3.8 wt %, to 75 μm with the same local solidification time, for a silicon content of 9.7 wt %. The rate of change is $-4.4\,\mu$m/% Si, whereas in Al–Cu alloys it changes from 98 μm for 3.5 wt % Cu to 58 μm for 9 wt % Cu,

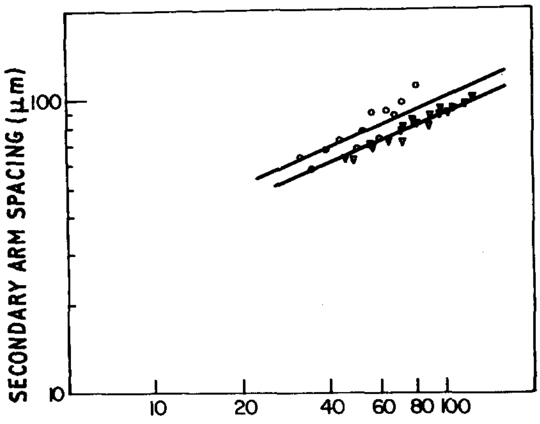

Figure 7 Dendritic arm spacing as a function of the local solidification time for A356 and Al–7.5% Si alloys. (○) A356, (▽) Al–7.5% Si.

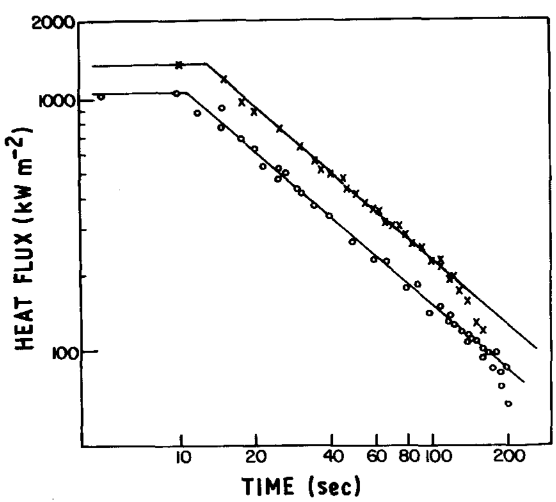

Figure 8 Heat flux as a function of time for Al–Cu alloys, for two initial chill temperatures. (×) 20° C, (○) 250° C.

i.e. $-7.3\,\mu m/\%$ Cu. Thus the element having lower solubility contributes more to the fineness of the structure than that with higher solubility. This finding is in accord with a previous research [4].

It is clear that the microstructure of the Al–7.5 wt % Si alloy is finer than that of the A356 alloy with the same local solidification time. This may be related to the presence of magnesium and a surface tension influence on the melt, affecting dendritic arm spacing, [5–7].

In castings made of A356 alloy the sodium and strontium contents were not checked. According to the manufacturer's data, a modification was made which induced a difference in the fineness of the silicon in the eutectic.

In all cases, however, the relationship $\lambda \sim t_f^{0.43}$ was found to hold. This value of n lies in the upper part of the interval $0.3 < n < 0.5$, quoted in the literature [1].

For controlled solidification of Al–4.4 wt % Cu, with the solidification rate and temperature gradient ahead of the solidification front determined independently of each other, the value $n = 0.31$ was found [8]. In the study of Bower *et al.* [9], an Al–4.5 wt % Cu ingot was solidified by cooling the bottom of an insulated cylinder, as in the present set-up, and the value found was $n = 0.39$, a deviation of only 10% from our result.

In solidification of succinonitrile–6 wt % camphor, migration of secondary arms over two or three spacings up the temperature gradient was observed [10]. This effect was explained by a temperature-gradient zone melting (TGZM) mechanism. The more time available for migration, the more intensive the coalescence and the coarser the structure. Small values of temperature gradient then lead to increases of the secondary arm spacing [10]. Under controlled solidification the temperature gradient, G, is constant, and spacing depends on the solidification time alone. Values of $n = 0.31$ are obtained as shown in the lower graph of Fig. 10. Both in the present experiment and those of Bower *et al.* [9], the temperature gradient varies with the distance from the cooling device, i.e. with the local solidification time. Decrease of the gradient under the TGZM mechanism, causes further coarsening of λ_2.

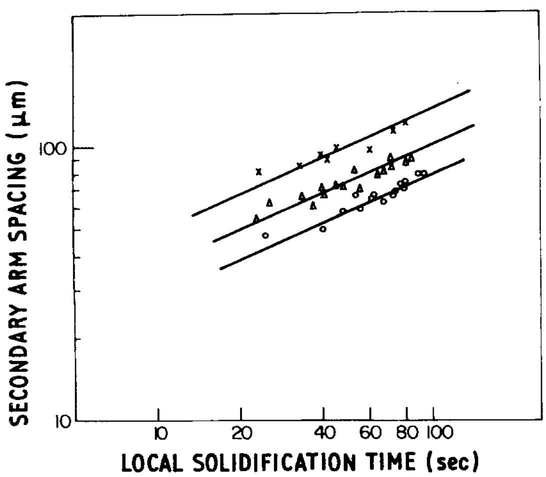

Figure 9 Dendritic arm spacing as a function of the local solidification time for Al–Cu alloy for three copper contents. (×) 3.5% Cu, (△) 4.6% Cu, (○) 9.0% Cu.

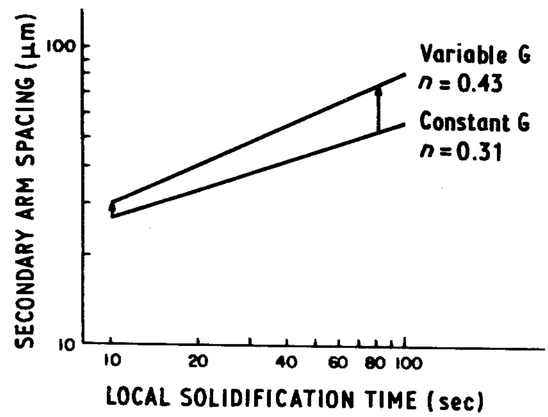

Figure 10 Schematic dependence between dendritic arm spacing and local solidification time.

At short solidification times the gradient is high and the λ_2 increment small, while at long times the gradient is low and the increment larger, resulting in the upper graph of Fig. 10. Thus under simultaneous variation of the gradient and the local solidification time, the resulting n value is higher than 0.31, as found both here and by Bower *et al.* [9]. Variations of the temperature gradient exist in profiled sections (but not in unidirectional solidification) – so that the results of experiments presented here may be more relevant to production conditions than those obtained under controlled solidification.

5. Conclusions

1. It was found that an experimental system comprising a computerized set-up using mathematical models for the analysis of cooling and solidification processes permits investigation of the heat flux to the chill, the cooling rates, and solidification times characterizing the casting process.

2. The heat flux from the casting to the chill depends on the initial temperature of the chill and on the properties of the cast material.

3. A mathematical model for solving the problem of the solidification behaviour of a cylindrical body was constructed, based on the heat flux from the casting to the chill and taking account of the temperature-dependent thermophysical properties of the cast material. The model yields results of an accuracy of 2 to 3% and permits calculation of the local solidification time.

4. It was found that the dendrite arm spacing is proportional to $t_f^{0.43}$, t_f being the local solidification time.

5. Raising the solute content leads to a finer microstructure for equivalent t_f. A low-solubility solute causes a finer structure than a high-solubility one.

6. The empirical formula for calculating dendritic arm spacing as a function of local solidification time enables structural fineness of the casting to be estimated directly from models for the calculation of the solidification parameters, which are themselves based on a mathematical analysis of casting conditions.

References

1. M. C. FLEMINGS, in "Solidification Processing"

(McGraw-Hill, New York, 1974) p. 146.
2. M. BAMBERGER, B. Z. WEISS and M. M. STUPEL, to be published.
3. M. HANSEN, in "Constitution of Binary Alloys", (McGraw-Hill, New York, 1968) pp. 84 and 132.
4. R. E. SPEAR and G. R. GARDNER, *Amer. Foundryman Soc. Trans.* **71** (1963) 209.
5. W. KURZ and D. J. FISHER, *Acta Metall.* **29** (1981) 11.
6. D. J. ALLEN and J. D. HUNT, in "Solidification and Casting of Metals", Proceedings of the Internation Conference on Solidification, Sheffield, 1977 (The Metals Society, London, 1979) Book 192 p. 39.
7. R. TRIVEDI and K. SOMBOONSUK, *Mater. Sci. Eng.* **65** (1984) 65.
8. K. P. YOUNG and D. H. KIRKWOOD, *Metall. Trans.* **6A** (1975) 197.
9. T. F. BOWER, H. D. BRODY and M. C. FLEMINGS, *Trans. Metall. Soc. AIME* **236** (1966) 624.
10. D. J. ALLEN and J. D. HUNT, *Metall. Trans.* **7A** (1976) 767.

Received 18 October 1984
and accepted 9 October 1985